Acta Physiologiae Plantarum (2023) 45:54
https://doi.org/10.1007/s11738-023-03528-5

ORIGINAL ARTICLE

Sandstorms damage the photosynthetic activities of *Haloxylon ammodendron* seedlings

Shengbo Shi[1,2] · Dangwei Zhou[2] · Rui Shi[3,4] · Tao Sun[1] · Fanglin Wang[1] · Xiuzhen Gao[2] · Yunian Zhang[1] · Peng Zhao[1] · Gaoxing Xu[1] · Jinnian Tang[1]

Received: 21 June 2021 / Revised: 7 April 2022 / Accepted: 8 February 2023 / Published online: 3 March 2023
© The Author(s) 2023

Abstract

Haloxylon ammodendron is a preferred shrub species for buffering against wind and fixing sand in arid sandy areas of northwest China. To determine whether sandstorms cause damage to *H. ammodendron* seedlings, we investigated the effects of wind-blown sands on the photosynthetic function of *H. ammodendron* by simulating sand-carrying wind in the wind tunnel. The results showed that photosystem II (PSII) non-photochemical quenching (*NPQ*) was sensitive to wind erosion, and sustained blowing of sand-carrying winds enhanced *NPQ* reduction. The rapidly relaxing quenching NPQ_f made up the majority component of *NPQ*; the NPQ_f/NPQ ratio was approximately 64.4% in the sand-free wind group and nearly 56.2% in the sand-carrying wind group. The distribution of the quantum efficiency of the excitation energy indicated that the relative proportions of the quantum yield of PSII photochemistry Φ_{PSII}, the quantum yield of quenching due to light-induced Φ_{NPQ}, and non-light-induced Φ_{NO} were influenced by both wind erosion and light intensity; the sand-carrying wind resulted in a relative decrease in Φ_{NPQ} and a corresponding increase in Φ_{NO}. The maximum quantum efficiency of PSII photochemistry F_v/F_m was relatively stable in the sand-free wind group, with an average value of approximately 0.81. Compared to sand-free wind, sand-carrying winds caused remarkable decreases in F_v/F_m. Light intensity was the main factor affecting Φ_{PSII}, Φ_{NPQ}, and relative electron transport rate (*rETR*); there was no interaction effect between the duration of sand-carrying wind and light intensity. Taken together, wind-blown sands cause irreversible damage to the photosynthesis of *H. ammodendron* seedlings, which is the main factor restricting population regeneration in shelterbelts.

Keywords *Haloxylon ammodendron* · Photosynthetic apparatus · PSII non-photochemical quenching · Sand-carrying wind · Self-renewal of artificial shelterbelt

Communicated by G. Bartosz.

✉ Shengbo Shi
sbshi@nwipb.cas.cn

Dangwei Zhou
dwzhou@nwipb.cas.cn

Rui Shi
shirui@berkgen.com

Tao Sun
suntaosuny@163.com

Fanglin Wang
wangfanglin2008@163.com

Xiuzhen Gao
gaoxz@nwipb.cas.cn

Yunian Zhang
aynal123@126.com

Peng Zhao
zhpg1987@sina.com

Gaoxing Xu
1569227904@qq.com

Jinnian Tang
tangjngs@126.com

[1] State Key Laboratory Breeding Base of Desertification and Aeolian Sand Disaster Combating, Gansu Desert Control Research Institute, Lanzhou, Gansu 730070, China

[2] Key Laboratory of Adaptation and Evolution of Plateau Biology, Northwest Institute of Plateau Biology, Chinese Academy of Sciences, Xining, Qinghai 810001, China

[3] School of Life Sciences, Sun-Yat-Sen University, Guangzhou, Guangdong 510275, China

[4] Guangdong Berkgen Biopharmaceuticals Co., Ltd., Shaoguan, Guangdong 512000, China

Abbreviations

F_v/F_m	Maximum quantum efficiency of PSII photochemistry at the open reaction center in the absence of *NPQ*
F_v^r/F_m^r	Maximum quantum efficiency of PSII photochemistry after 15 min of dark relaxation
NPQ	PSII non-photochemical quenching
NPQ_f	Rapidly relaxing quenching of *NPQ*
NPQ_s	Slowly relaxing quenching of *NPQ*
PPFD	Photosynthetic photon flux density
PSII	Photosystem II
q_L	Fraction of the open PSII reaction center
q_{NP}	PSII non-photochemical quenching coefficient
rETR	Relative electron transport rate of the PSII reaction center
$rETR_{max}$	Maximum relative electron transport rate of the PSII reaction center
Φ_{NO}	Quantum yield of non-regulatory energy dissipation in the PSII reaction center
Φ_{NPQ}	Quantum yield of regulatory energy dissipation in the PSII reaction center
Φ_{PSII}	Quantum yield of PSII photochemistry at a given light intensity, also termed as PSII operating efficiency

Introduction

China is one of the countries in the world that face serious desertification, with large areas of desertified land in northwest, western northeast, and northern North China (Wang et al. 2006; Zhao and Sun 2013; Chen et al. 2018). The stable development of the regional economy has been restricted by environmental degradation and desertification (Dong et al. 2004; Zhang et al. 2010; Wan and Yan 2018). Sandstorms, however, intensify the process of land desertification (Xu et al. 2002). As a severe weather disaster, sandstorms occur frequently in arid and desert areas and can cause serious losses to the ecological environment, industry, and agriculture (Shi et al. 2000; He et al. 2021). Arid and desert areas of China are drastically affected by sandstorms almost every year, especially in early spring (Qian et al. 2002; Ma et al. 2019).

Building artificial shelterbelts at the edge of deserts is a cost-effective way to prevent and control desertification (Qu et al. 2019). The Hexi Corridor in Gansu Province, China has a long history of combating desertification, which can be traced back at least 400 years to sporadic civil activity. Beginning in the 1950s, a variety of prevention and control measures were developed, such as combining species of trees and bushes, and dune afforestation was successful. However, since the mid-1980s, *Haloxylon ammodendron* and other artificial dune forests in the Hexi sand area began to shrink and perished on a large scale (Wang and Ma 2003); adult artificial forests face a vanishing phenomenon that is difficult to self-renew naturally.

A forest of *H. ammodendron* in Minqin undergoes natural renewal (Guo et al. 2005). Ding et al. (2011) found that compared to the natural *H. ammodendron* forest, artificial forests had greater aggregation among seedlings; they argued that less uniformity in the spatial distribution of juvenile seedlings can greatly affect the natural regeneration of these plantations. However, others believe that the aggregative distribution pattern in adult *H. ammodendron* forests can adapt to harsh environments, which is conducive to the survival and reproduction of individuals (Song et al. 2010; Su et al. 2019). Bormann and Likens (1981) considered that the survival of the population requires not only a suitable habitat environment but also a sufficient number to reach the minimum population density; an insufficient number of progeny and recruitment from seedlings into adults may limit the self-renewal of plant populations and even lead to their degeneration (Edelfeldt et al. 2019).

The growth and development of plants are not only affected by their biological characteristics but also restricted by their living environment. It is generally believed that when a plant population is in a disadvantageous habitat for a long time, its number can show a persistent decline, eventually leading to shrinkage or even the extinction of the population (Wang and Li 2008). Field investigation and observation show that few juvenile seedlings survive in the adult *H. ammodendron* shelterbelt, and the population age structure showed a declining trend. It is obvious that the difficulty of replenishing seedlings restricts sustainability and increases in population size, directly affecting its renewal. We speculate that the strong and frequent early spring sandstorms in the *H. ammodendron* shelterbelt area cause irreversible damage to green assimilative branches, making it difficult for juvenile seedlings to survive; a shortage of a sufficient number of progeny and recruitment from seedlings can directly affect the regeneration of the plant population and cause its shrinkage.

Haloxylon ammodendron is a remnant of the ancient Mediterranean flora and is mainly distributed in desert areas with low rainfall (30–200 mm) in Africa and Asia, and has been widely cultivated in mobile dunes, semi-fixed dunes and fixed sand dunes of the oasis edge of Minqin region (Wang and Ma 2003). Hu et al. (2021) analyzed the relationship of the morphological and photosynthetic characteristics in *H. ammodendron* in the four habitats of the Ebinur Lake wetland, and they found that in high-water and high-salt habitats, photosynthesis is affected by "stomata restriction", while in other habitats, photosynthesis is mainly affected by "non-stomata restriction". Photosynthesis is also affected by wind-blown sand, especially in herbs, whereas shrubs have a better resistance to strong winds (Yu et al. 2002). Thus, we

proposed the following hypotheses: although *H. ammodendron* is an excellent windproof and sand-fixing plant species in arid and desert areas, the tender assimilative branches are sensitive to wind-blown sand; sandstorm blowing leads to irreversible damage to photosynthetic activities, which makes it difficult for seedlings to survive and causes a lack of progeny supply and restricts self-renewal of the population.

In this report, we simulated the blowing of sand-carrying wind in a wind tunnel to study the effects of wind-blown sands on the function of the photosynthetic apparatus of *H. ammodendron* seedlings. We analyzed the variations in photosystem II (PSII) photochemical efficiency and the quantum yield of energy dissipation in the PSII reaction center. We also observed the configuration of plants in fields and morphological characteristics of epidermal tissues of green assimilative branches. We conclude that wind-blown sands cause irreversible damage to the photosynthesis of *H. ammodendron* seedlings, which is the major reason restricting population regeneration in shelterbelts.

Materials and methods

Cultivation of seedlings and simulation of sand-carrying winds in a wind tunnel

Simulation experiments of the blowing of sand-free wind and sand-carrying wind were performed in the wind tunnel at the State Key Laboratory Breeding Base of Desertification and Aeolian Sand Disaster Combing, Gansu Province, China. Fine sand was collected from dunes near the Gansu Minqin National Studies Station for Desert Steppe Ecosystem, filtered through a wire gauze screen, and then blown several times in the wind tunnel to remove dust. The average particle size of sand grains is approximately 220 μm. The wind tunnel in the wind-sand environment is designed with direct current blowing. The total length of the tunnel is approximately 39.8 m; among them, the length of the test section is 16 m and that of the moving section is 2 m, and the cross-section is 1.2 × 1.2 m. The simulated wind speed ranges from 4 to 35 m/s, and the accuracy is ± 3.0–0.5% (Sun et al. 2021).

Two-year-old potted *H. ammodendron* seedlings were used for the wind erosion simulation. In early May 2017, seedlings were raised in the nursery of Wuwei State Key Laboratory Breeding Base with seeds collected from the artificial forest around the Minqin field station the previous year. The cultivation substrate was mixed in a ratio of soil to sand of 1:9; a small amount of organic fertilizer was added to ensure that the seedlings obtained the nutrients they needed to grow. Deep plastic pots with an opening diameter of 22 cm and height of 45 cm were used (near 15 L), and approximately 10 seeds per pot were sown. The pots were buried approximately 40 cm deep in one plot of 5 m × 8 m with good natural ventilation and lighting; all pots were arranged in 5 rows in the east–west direction, the spacing between pots was approximately 8 cm in each row, and the row spacing was approximately 50 cm. Normal field management was performed as the plants grew; the seedlings were thinned to four or five per pot when they grew to approximately 5 cm in height. In August and September 2018, healthy biennial seedlings with a relatively consistent plant configuration were chosen for the wind erosion simulation experiments. The plants were divided into two groups: the sand-free wind group and the sand-carrying wind group. Pots of plants in the sand-free wind group were placed approximately 1.5 m in front of sand laying in the test section of the wind tunnel, and the sand-carrying wind group was placed in the moving section after sand paving. The platform in the moving section can be adjusted up and down to fit most of tender branches within a height of 30 cm. The wind speed was set at 12 m/s with a sediment transport rate of approximately 45 g/cm^2 within a height of 20 cm (Sun et al. 2021), and the blowing time was 10, 20, or 40 min. Similar trials were performed in 2019 using seedlings cultured in 2017 and 2018.

Chlorophyll fluorescence imaging

After completing the wind erosion simulation in the wind tunnel, the flowerpots were placed under a semi-shaded tree with scattered light of a photosynthetic photon flux density (PPFD) of approximately 400 ± 100 μmol photons m^{-2} s^{-1} to avoid direct sunlight. A small handheld hairdryer was used to blow the whole plant quickly to remove fine sand particles clinging to the surface of the branches. Then, branches growing at similar heights and positions with no visible damage were selected from various treatment plants. Chlorophyll fluorescence was measured with a chlorophyll fluorescence image analyzer (CF-imager, Technologica Ltd, Essex, United Kingdom) equipped with a light emitting diode (LED) red and blue light source. Green assimilative branches approximately 6 cm long were cut and picked from seedlings. The segments of branches were set on the imaging platform and fixed with a nylon fishing line 0.09 mm in diameter; a sufficiently moistened cotton pad was laid under the samples. After imaging and focusing of the charge coupled device (CCD) camera, the preset protocol was operated. The room temperature was maintained at approximately 18.0 ± 1.0 °C, and the relative air humidity was approximately 40 ± 2% during the measurement period.

Determination of chlorophyll fluorescence parameters

Determination of steady-state PSII photochemical efficiency: The built-in protocol was divided into two parts: slow induction kinetics and dark relaxation (dark recovery).

After the green branches adapted in the dark for 15 min, the initial fluorescence (F_o) and maximal fluorescence (F_m) were determined. Actinic lights of 400 and 1500 μmol photons m^{-2} s^{-1} (represented by LL and HL, respectively) were successively irradiated for 15 min, and steady-state fluorescence (F_s) and maximal fluorescence (F_m') were determined. Then, the actinic lights were turned off, dark relaxation was restored for 15 min, and minimal fluorescence F_o^r and maximal fluorescence F_m^r were measured in sequence at 5, 10, and 15 min. Saturated pulsed lights for measuring F_m, F_m', and F_m^r were set to 6840 μmol photons m^{-2} s^{-1} and lasted for 60 ms.

Measurement of the rapid light response curve: refer to the method of Baker and Rosenqvist (2004). After darkening adaptation for 15 min, the F_o and F_m of the green assimilative branches of the seedlings were determined. Then, the branches were irradiated with 400 μmol photons m^{-2} s^{-1} low steady-state actinic light for 10 min, and the light response curve was measured. We obtained F_s and F_m' at each light intensity gradient of 25, 50, 100, 150, 200, 300, 500, 800, 1000, 1200, 1500, and 1800 μmol photons m^{-2} s^{-1}. Saturated pulsed lights for determining F_m and F_m' were set to 6840 μmol photons m^{-2} s^{-1} and lasted for 60 ms. According to the variation in F_s, the equilibrium time was 2 min at light intensities of 25, 50, 100, and 150 μmol photons m^{-2} s^{-1} and 1 min above 200 μmol photons m^{-2} s^{-1}.

Localization and fluorescence imaging

In the graphic editing frame of the fluorescence image, the assimilative branch images from the sand-free wind group and sand-carrying wind group were separated by blowing time (10, 20, and 40 min). The parameter values of the fluorescence images of each assimilative branch were resolved one by one, and then the data were copied to an Excel spreadsheet for further analysis.

Analysis of PSII photochemical efficiency and non-photochemical quenching

The maximum quantum efficiency of PSII photochemistry (F_v/F_m) was calculated from F_o and F_m of the dark-adapted leaf, where $F_v = F_m - F_o$. The maximum quantum efficiency of PSII photochemistry after 15 min of dark relaxation was expressed as F_v^r/F_m^r; $F_v^r = F_m^r - F_o^r$, the minimal fluorescence F_o^r, and the maximal fluorescence F_m^r were obtained after dark relaxation for 5, 10, and 15 min in sequence.

The quantum yield of PSII photochemistry at a given light intensity Φ_{PSII} was calculated according to the formula of Genty et al. (1989): $\Phi_{PSII} = (F_m' - F_s)/F_m'$. The quantum yields of non-regulatory and regulatory energy dissipation in the PSII reaction center, Φ_{NO} and Φ_{NPQ}, were calculated by $\Phi_{NO} = 1/(NPQ + 1 + q_L \times [F_m/F_o - 1])$ and $\Phi_{NPQ} = 1 - \Phi_{PSII} - 1/(NPQ + 1 + q_L \times [F_m/F_o - 1])$, respectively (Kramer et al. 2004). Here, q_L is the fraction of the open PSII reaction center estimated with Baker's (2008) method, $q_L = ([F_m' - F_s]/[F_m' - F_o']) \times (F_o'/F_s)$.

The relative electron transport rate *rETR* of the PSII reaction center was calculated as follows: $rETR = \Phi_{PSII} \times PPFD \times 0.5 \times 0.84$, where 0.84 represents the average proportion of light absorbed by the leaf and 0.5 is the fraction of light absorbed by PSII (assuming an equal distribution between PSII and PSI).

PSII non-photochemical quenching (*NPQ*) was calculated according to the formula of Bilger and Björkman (1990): $NPQ = F_m/F_m' - 1$. The PSII non-photochemical quenching ability was also expressed as the quenching coefficient q_{NP}, defined as the PSII non-photochemical quenching coefficient and was calculated from the equation, $q_{NP} = 1 - (F_m' - F_o')/(F_m - F_o)$ (Quick and Stitt 1989). The rapidly relaxing quenching (NPQ_f) and slowly relaxing quenching (NPQ_s) of PSII non-photochemical quenching were estimated according to Maxwell and Johnson (2000): $NPQ_s = (F_m - F_m^r)/F_m^r$; $NPQ_f = (F_m/F_m') - (F_m/F_m^r)$, where F_m and F_m^r are the maximal fluorescence after 15 min of dark adaptation and dark relaxation, respectively.

In the above calculation, F_o' was estimated from the empirical formula of Oxborough and Baker (1997): $F_o' = F_o/(F_v/F_m + F_o/F_m')$, where F_o and F_m are minimal and maximal fluorescence after dark adaptation for 15 min.

Observation of morphology and scanning electron microscope

After the completion of the simulation trials in the wind tunnel, all pots of seedlings were promptly carried back to the nursery, placed in the original position, and buried at a depth of approximately 40 cm. On the first, second, and third days of the wind erosion trials, morphological changes were continuously observed; visible injury to the windward and corresponding leeward sides of branches was recorded with a digital camera.

At the same time, on the second and third days of wind erosion, we collected tender branches with no obvious harm from different treatments and cut them into small segments with lengths of approximately 1 cm. After being glued behind the sample platform, the surface structure of epidermal tissue was scanned and observed using a TM4000 Hitachi table scanning electron microscope (Hitachi High-Technologies Corporation, Japan).

Statistical analysis

The data were first sorted in Microsoft Excel and then analyzed statistically with SPSS Version 16.0. Independent-samples *T* tests were used to analyze differences between

the sand-free wind group and the sand-carrying wind group. Multivariate analysis of variance was used to compare the significance of differences in wind erosion times, and the least significant difference method was used for multiple comparisons, with the significance level set at $\alpha = 0.05$. The interactive effect of light intensity and wind erosion time was analyzed by multivariate general linear modeling (GLM). Data in figures are means, the vertical bars are standard deviations, and the number of samples is 12.

Results

Effects of wind erosion on the relative electron transport rate of the PSII reaction center

The light response curves of green assimilative branches of *H. ammodendron* seedlings showed that the PSII relative electron transport rate (*rETR*) increased logarithmically as the photosynthetic photon flux density (PPFD) increased. The *rETR* curves increased rapidly when the PPFD was less than 300 μmol photons m^{-2} s^{-1} and increased slowly after more than 800 μmol photons m^{-2} s^{-1} (Fig. 1). The initial slopes of the *rETR* light curves (α) in the sand-free wind group were 0.266, 0.276, and 0.277 at 10, 20, and 40 min, respectively; the PSII maximum relative electron transport rates ($rETR_{max}$) at 1800 μmol photons m^{-2} s^{-1} were 143.45 ± 5.36, 152.05 ± 9.38, and 144.60 ± 4.70 μmol electrons m^{-2} s^{-1}, respectively. In the sand-carrying wind group, α was 0.274, 0.251, and 0.258, and $rETR_{max}$ was 147.60 ± 7.18, 135.55 ± 9.50, and 139.66 ± 9.74 μmol electrons m^{-2} s^{-1}, respectively.

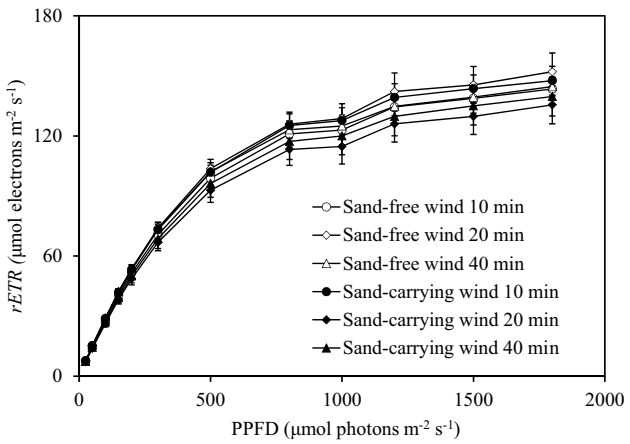


Fig. 1 Light response curves of the PSII relative electron transport rate (*rETR*) after 12 m/s sand-free wind and sand-carrying wind blowing for 10, 20, and 40 min on green branches of *H. ammodendron*. Each data point represents the mean of 12 samples

Figure 2 shows that there was an increasing trend of *rETR* with prolongation of sand-free wind erosion; after irradiation at 1500 μmol photons m^{-2} s^{-1} high steady-state actinic light intensity (HL) for 20 and 40 min, the *rETR* value was prominently higher than that at 10 min ($p < 0.05$), but there was no obvious difference at 400 μmol photons m^{-2} s^{-1} low light intensity (LL). However, in the sand-carrying wind group, the *rETR* values at 20 and 40 min were remarkably lower than those at 10 min ($p < 0.05$). There was no difference between the sand-free wind and the sand-carrying wind groups when blowing for 10 min; with sustained blowing of wind erosion for 20 and 40 min, the *rETR* of the sand-carrying wind group was remarkably lower than that of the sand-free wind group at both HL and LL ($p < 0.01$ and $p < 0.001$).

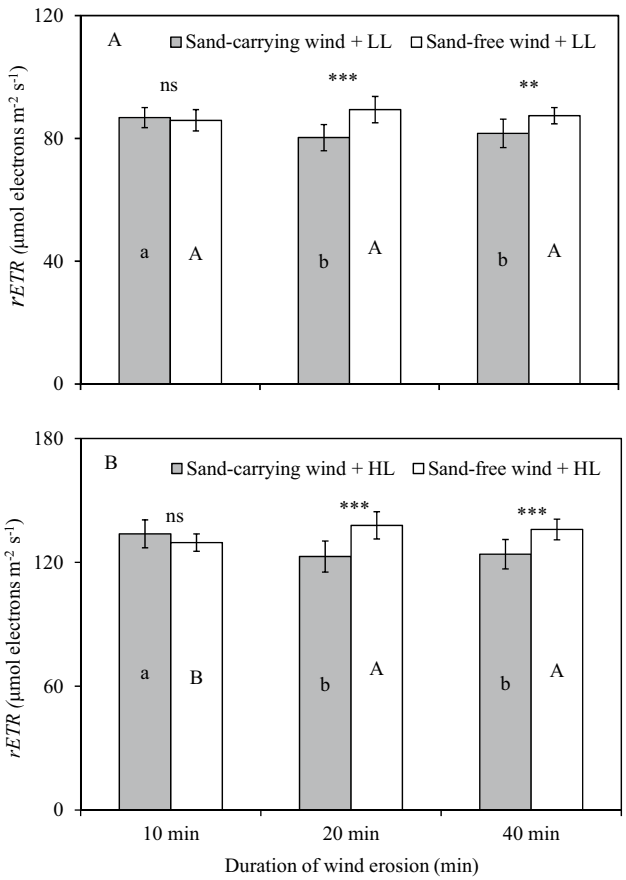


Fig. 2 Effects of 12 m/s sand-free wind and sand-carrying wind on the PSII relative electron transport rate (*rETR*) in green branches of *H. ammodendron* after irradiation at high and low steady-state light intensities for 15 min each by time (10, 20, and 40 min of wind erosion). Different uppercase and lowercase letters indicate a significant difference in *rETR* among 10, 20, and 40 min of wind erosion time for sand-free wind and sand-carrying wind, respectively ($\alpha = 0.05$). "*ns*" indicates no significant difference ($p > 0.05$), ** and *** indicate a highly significant difference ($p < 0.01$ and $p < 0.001$) between sand-free wind and sand-carrying wind

Response of the PSII non-radiative energy dissipation to blowing of wind erosion

The light response curve of the PSII non-photochemical quenching coefficient (q_{NP}) showed that it increased logarithmically with increasing PPFD in both the sand-free wind group and the sand-carrying wind group. The light curves of q_{NP} increased rapidly when PPFD was less than 100 μmol photons m^{-2} s^{-1} and slowly after more than 300 μmol photons m^{-2} s^{-1}; from 100 to 300 μmol photons m^{-2} s^{-1} was the transition range for q_{NP}. Although there was no difference in the wind-only group, the q_{NP} showed an obvious decreasing tendency with blowing time in the sand-carrying wind group, and its curves were also lower than those from the sand-free wind group (Fig. 3).

Further studies indicated that when irradiated with HL for 15 min, wind-blown sand led to prominent decreases (10 min, $p < 0.05$; 20 min, $p < 0.01$; 30 min, $p < 0.001$) in PSII non-photochemical quenching (*NPQ*) compared to the wind-only group (Fig. 4C). Over time, both sand-free wind and sand-carrying wind caused a decrease in *NPQ*; this was more marked in the sand-carrying wind group, which showed a remarkable difference between 10 and 40 min ($p < 0.05$). Similar tendencies were also found in LL (not shown in the figure).

After dark relaxation for 15 min, the relative change in the rapid and slow relaxation quenching in the PSII reaction center (NPQ_f and NPQ_s) showed that the NPQ_f component accounted for a large proportion of *NPQ*; the average NPQ_f/NPQ after the blowing of sand-free wind and sand-carrying wind was 64.4% and 56.2%, respectively (Fig. 4A and B). There was little difference in NPQ_f by blowing time in the sand-free wind group; however, when blowing for 20 and 40 min, NPQ_f was obviously lower than that for 10 min in the sand-carrying wind group ($p < 0.05$). Compared to wind-only group, the relative reductions in NPQ_f and NPQ_s

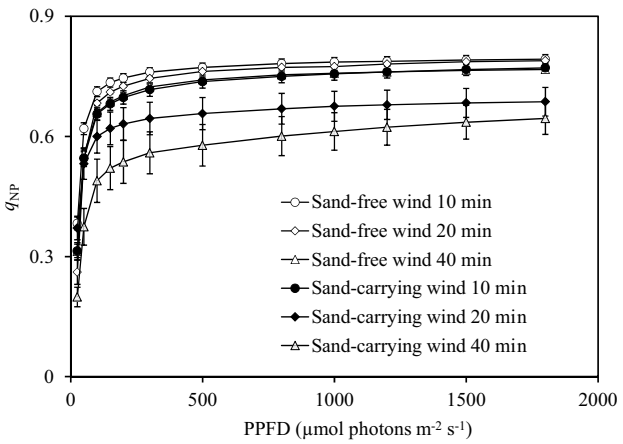


Fig. 3 Light response curves of the PSII non-photochemical quenching coefficient (q_{NP}) after 12 m/s sand-free wind and sand-carrying wind blowing for 10, 20, and 40 min on green branches of *H. ammodendron*. Each data point represents the mean of 12 samples

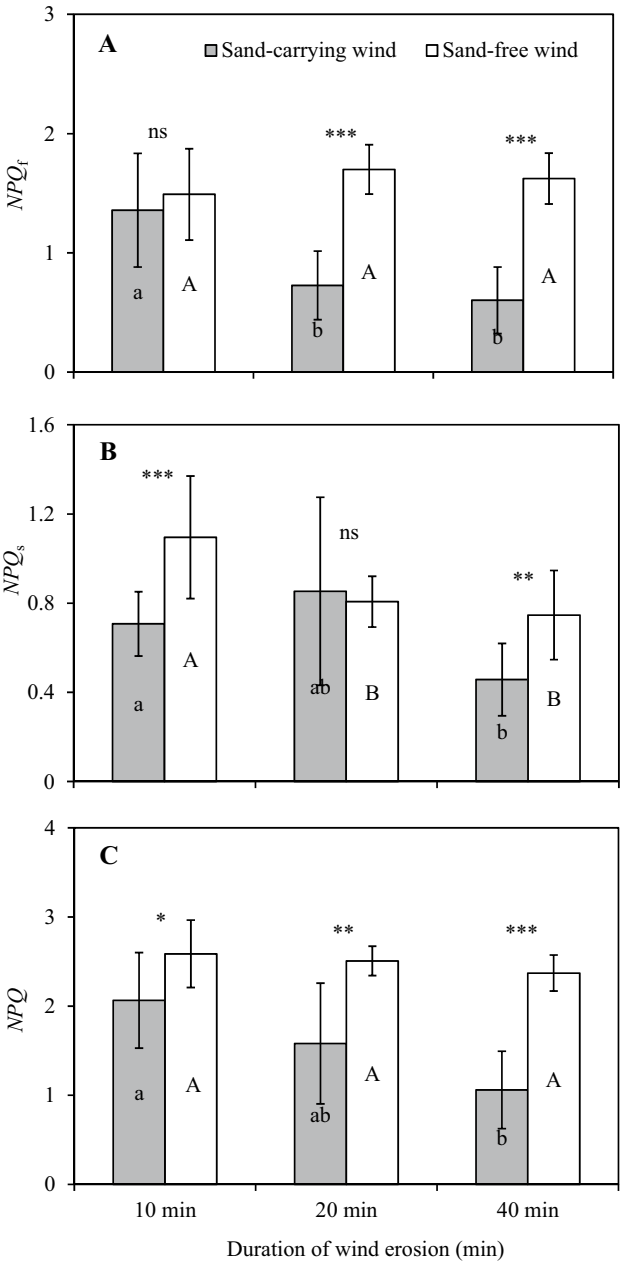


Fig. 4 Effects of 12 m/s sand-free wind and sand-carrying wind on PSII non-photochemical quenching (*NPQ*) and its rapidly and slowly relaxing quenching (NPQ_f and NPQ_s) in green branches of *H. ammodendron* after irradiation at high and low steady-state light intensity for 15 min each. Different uppercase and lowercase letters indicate a significant difference in *NPQ*, NPQ_f, and NPQ_s among 10, 20, and 40 min of wind erosion time for sand-free wind and sand-carrying wind, respectively ($\alpha = 0.05$). "*ns*" indicates no significant difference ($p > 0.05$), * indicates a significant difference ($p < 0.05$), ** and *** indicate a highly significant difference ($p < 0.01$ and $p < 0.001$) between sand-free wind and sand-carrying wind

caused by wind-blown sand were approximately 44.2% and 22.4%, respectively.

Effects of wind erosion on photochemical and non-photochemical quantum efficiency distribution of excitation energy in the PSII reaction center

There are photochemical and non-photochemical dissipation pathways of the excitation energy accumulated in the PSII reaction center (Kramer et al. 2004). Figure 5A and B indicate that after sand-carrying wind was blown for different amounts of time, the quantum yield of PSII photochemistry (Φ_{PSII}) showed a similar change tendency at HL and LL; in other words, except for 10 min, sustained blowing of sand-carrying wind for 20 min and 40 min caused a remarkable decrease in Φ_{PSII} ($p < 0.05$). However, in the sand-free wind group, Φ_{PSII} was slightly lower after blowing for 10 min than 20 min and 40 min, and the difference was only obvious under HL irradiation ($p < 0.05$).

The variation in the PSII quantum yield of non-regulatory energy dissipation (Φ_{NO}) showed consistent variation after the blowing of sand-free wind and sand-carrying wind for different amounts of time (Fig. 5C and D). With prolongation of blowing time, Φ_{NO} increased gradually in the sand-carrying wind group; there was an obvious difference between 10 and 40 min ($p < 0.05$). However, in the sand-free wind group, the Φ_{NO} value increased slightly, with no obvious difference among the durations of each blowing ($p > 0.05$); the average Φ_{NO} was 0.175 at LL and 0.227 at HL.

The PSII quantum yield of regulatory energy dissipation (Φ_{NPQ}) was sensitive to PPFD; its values were obviously lower at LL than at HL (Fig. 5E and F). After the blowing of sand-free wind and sand-carrying wind, Φ_{NPQ} showed consistent variation under both LL and HL irradiation. In other words, the Φ_{NPQ} value decreased gradually with blowing time, and the difference between 10 and 40 min was prominent ($p < 0.05$).

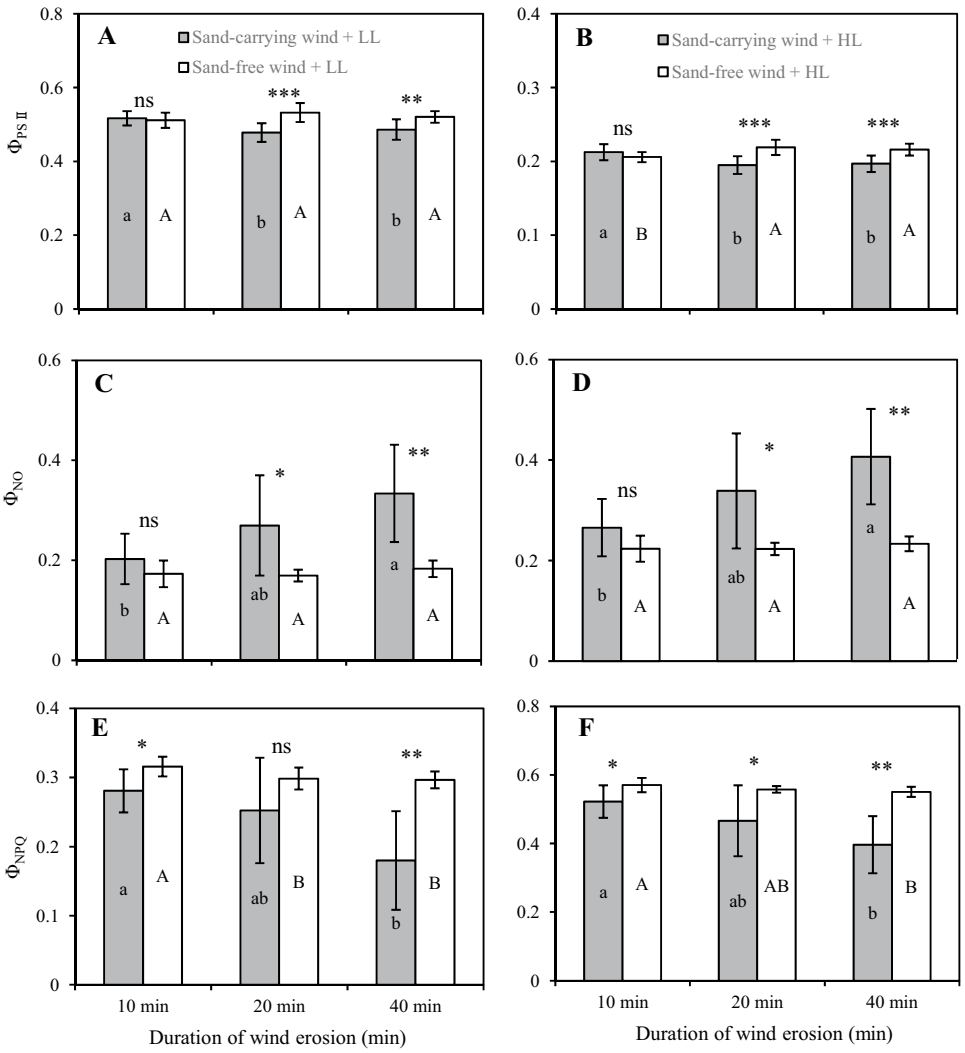


Fig. 5 Effects of 12 m/s sand-free wind and sand-carrying wind on PSII actual photochemical quantum efficiency (Φ_{PSII}), the quantum yield of quenching due to non-light-induced process (Φ_{NO}), and light-induced process (Φ_{NPQ}) in green branches of *H. ammodendron* after irradiation at high and low steady-state light intensity for 15 min each. Different uppercase and lowercase letters indicate a significant difference in Φ_{PSII}, Φ_{NO}, and Φ_{NPQ} among 10, 20, and 40 min of wind erosion time for sand-free wind and sand-carrying wind, respectively ($\alpha = 0.05$). "*ns*" indicates no significant difference ($p > 0.05$), * indicates a significant difference ($p < 0.05$), ** and *** indicate a highly significant difference ($p < 0.01$ and $p < 0.001$) between sand-free wind and sand-carrying wind

Limitation of wind erosion on the maximum quantum efficiency of PSII photochemistry and its dark relaxation

Figure 6B shows that the maximum quantum efficiency of PSII photochemistry (F_v/F_m) was relatively stable in the sand-free wind group, with an average value of approximately 0.81. The value of F_v/F_m in the sand-carrying wind group decreased gradually with prolongation of blowing time, showing an obvious difference between 10 and 40 min ($p<0.05$). Compared to the sand-free wind, F_v/F_m in the sand-carrying wind group decreased obviously (10 min, $p<0.05$; 20 min, $p<0.01$; and 40 min, $p<0.001$).

The maximum quantum efficiency of PSII photochemistry after 15 min of dark relaxation, F_v^r/F_m^r, was lower in both the sand-free wind and sand-carrying wind groups; it was not restored to the F_v/F_m level of the corresponding dark adaptation (Fig. 6A). After blowing for 20 and 40 min, F_v^r/F_m^r in the sand-free wind group was obviously higher than that at 10 min ($p<0.05$), whereas in the sand-carrying wind group it was obviously lower than that at 10 min ($p<0.05$). F_v^r/F_m^r in the sand-carrying wind group was remarkably lower at 20 min and 40 min than the corresponding values in the sand-free wind group ($p<0.001$ and $p<0.01$), but there was no difference at 10 min.

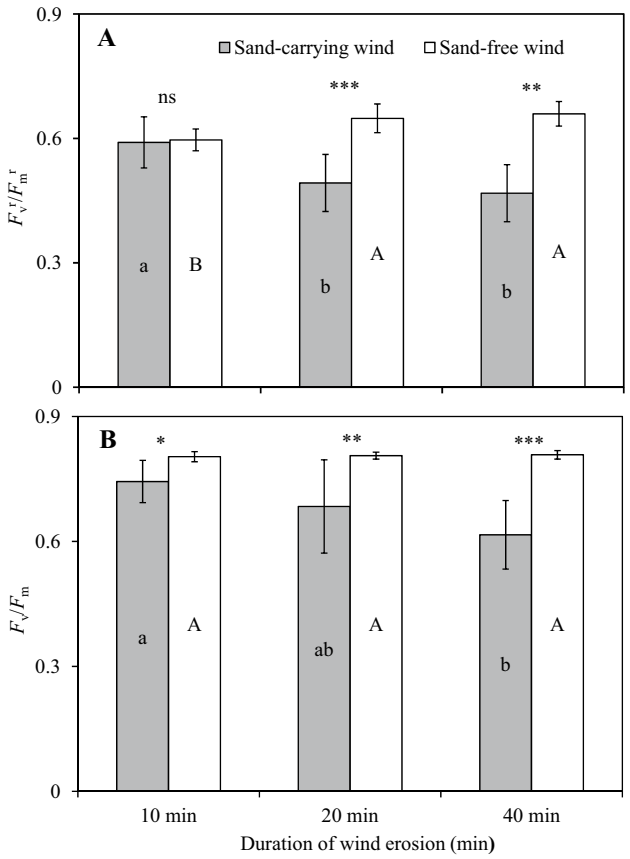


Fig. 6 Effects of 12 m/s sand-free wind and sand-carrying wind on the maximum quantum efficiency of PSII photochemistry (F_v/F_m) after dark adaptation for 15 min and the maximum quantum efficiency of PSII photochemistry (F_v^r/F_m^r) after dark relaxation for 15 min when actinic light irradiation is turned off in green branches of *H. ammodendron*. Different uppercase and lowercase letters indicate a significant difference in F_v/F_m and F_v^r/F_m^r among 10, 20, and 40 min of wind erosion time for sand-free wind and sand-carrying wind, respectively ($\alpha=0.05$). "*ns*" indicates no significant difference ($p>0.05$), * indicates a significant difference ($p<0.05$), ** and *** indicate a highly significant difference ($p<0.01$ and $p<0.001$) between sand-free wind and sand-carrying wind

Configuration of *H. ammodendron* plants and damage to the tender assimilative branches

The configuration of *H. ammodendron* growing under field natural conditions is mostly variable because of the long-term impact of sandstorms and other environmental adversities. Figure 7A shows that adult plants had almost no green assimilative branches near the ground; juvenile branches at the top of the canopy were sometimes dry and damaged (Fig. 7B). After being subjected to 12 m/s sand-carrying wind for 20 min, the tender green branches of the seedlings showed some changes the day later. In addition to being slightly withered and dead, tender branches often showed lignified spots; the windward side tended to become darker and was more prone to damage spots (Fig. 8).

Scanning observations indicated that the green assimilative branches could conglutinate dust on both the windward side and leeward side, and the control plant without wind erosion treatment also had small dust grains on the green branches (Fig. 9).

Discussion

Photosynthesis, as an important physiological process of plants, is very sensitive to changes in the environments (De Roo et al. 2020). The PSII relative electron transport rate (*rETR*) reflects the total capacity of plants for photosynthetic transfer (Maxwell and Johnson 2000; Pleban et al. 2020) and should also be influenced by wind erosion. However, The variation in the *rETR* of the rapid light response curve in *H. ammodendron* seedlings was similar after the blowing of sand-free wind and sand-carrying wind, and there were no obvious differences among the three typical blowing periods; even the so called negative impact of wind-blown sand was very small (Fig. 1). Rapid light curves can characterize the steady-state light acclimation status of a plant (Serôdio et al. 2006). Although the rapid light response curves of the *rETR* seem little affected by the wind erosion and its duration, the experiments conducted under 400 μmol photons m^{-2} s^{-1} low light intensity (LL) and 1500 μmol photons m^{-2} s^{-1} high light intensity (HL) provided a more prominent

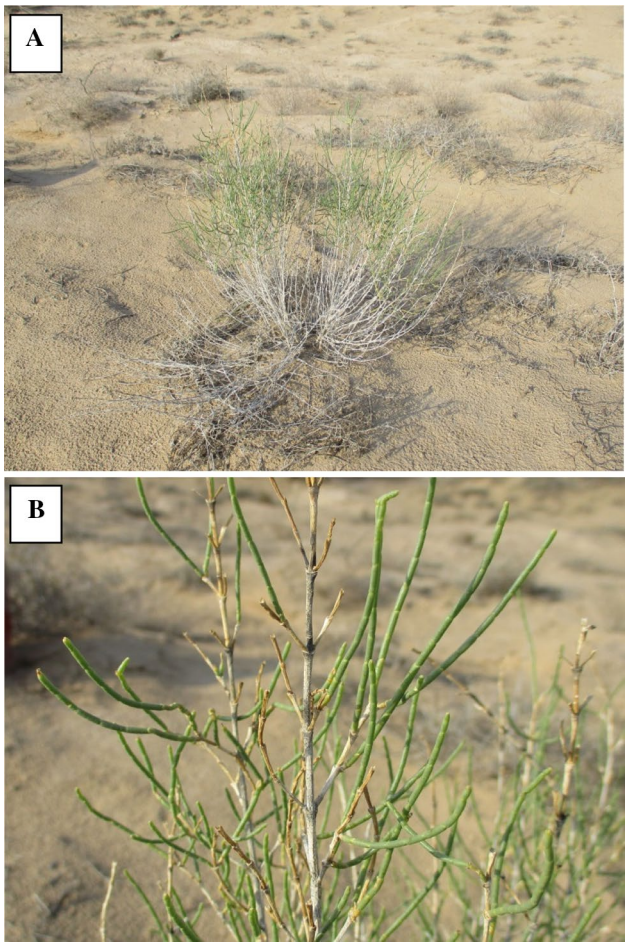


Fig. 7 *H. ammodendron* growing in natural environments and its green assimilative branches in the canopy

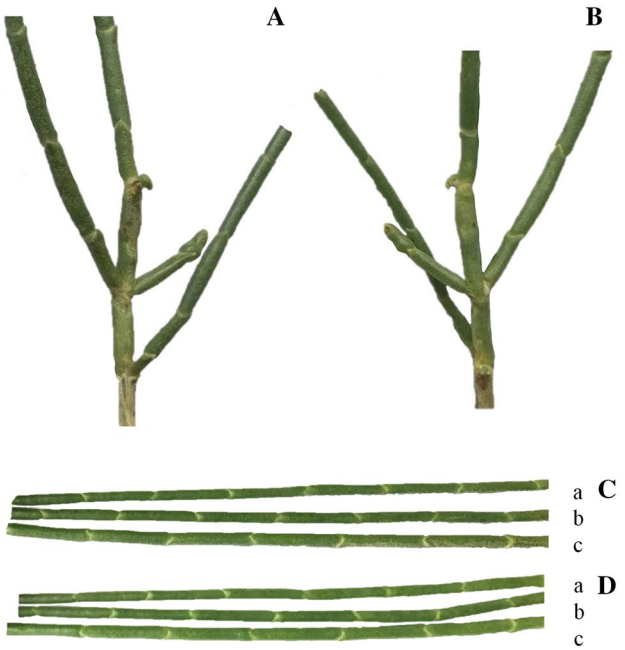


Fig. 8 Comparison of injury to epidermal tissue on the windward and leeward sides of green assimilative branches of *H. ammodendron* seedlings after blowing of 12 m/s sand-carrying wind for 15 min. The twig in panel A is from the windward side, and the twig in panel B is from the leeward side of the same site of the same plant. Identical lowercase letters in panels C and D indicate the windward and leeward sides of the same branch of *H. ammodendron* seedlings; the right end of the segments in panels C and D is toward the base of the assimilative branches, and the left end is toward the top of the branches. Photos were taken the day after exposure to sand-carrying wind

result (Fig. 2). This indicates that there was no negative impact of sand-free wind on the linear (acyclic) electron transfer process in the PSII reaction center, and only sand-carrying wind restricted and obstructed the electron transfer capacity of *H. ammodendron* seedlings. No difference was found when the blowing of sand-free wind and sand-carrying wind lasted 10 min; it is possible that such a short time of wind-blown sand did not cause sufficient impact to green assimilative branches, and the total photosynthetic electron transfer capacity of the photosynthetic apparatus was not greatly affected. There was no further decrease in *rETR* after 40 min of sand-carrying wind, and the slight increase in *rETR* after 20 and 40 min of sand-free wind was probably due to the compensating and overcompensating effects of photosynthetic function after the removal of adversity (Dyer et al. 1991; Gaudet and Keddy 1998; Masini et al. 2019).

The non-photochemical quenching of the PSII reaction center, also called "non-radiative energy dissipation", can consume excess light energy absorbed by leaves, thus preventing photo-damage to the photosynthetic apparatus (Niyogi and Truong 2013); it has been considered a regulatory process by which plants actively respond to stress in the external environment (Štroch et al. 2008). The non-photochemical quenching ability of *H. ammodendron* seedlings was sensitive to sand-free wind, especially sand-carrying wind. The light response curve of the PSII non-photochemical quenching coefficient (q_{NP}) clearly indicated that it decreased slightly with blowing time in the sand-free wind group but decreased obviously in the sand-carrying wind group (Fig. 3). It is clear that sustained strong wind erosion can inhibit the non-photochemical quenching process and reduce the plant's ability to dissipate excess light energy, so it was difficult to avoid damage to the functional PSII reaction center, especially with wind-blown sand. Calculating PSII non-photochemical quenching (*NPQ*) does not require the minimum chlorophyll fluorescence yield F_o', which can show obvious variation in the higher light intensity range and is a sensitive reflection of thermal dissipation capacity (Baker 2008). The experiment with steady-state actinic light intensity further confirmed that wind-blown sand aggravated the reduction in *NPQ* of *H. ammodendron* seedlings, with the reduction more remarkable with prolongation of blowing

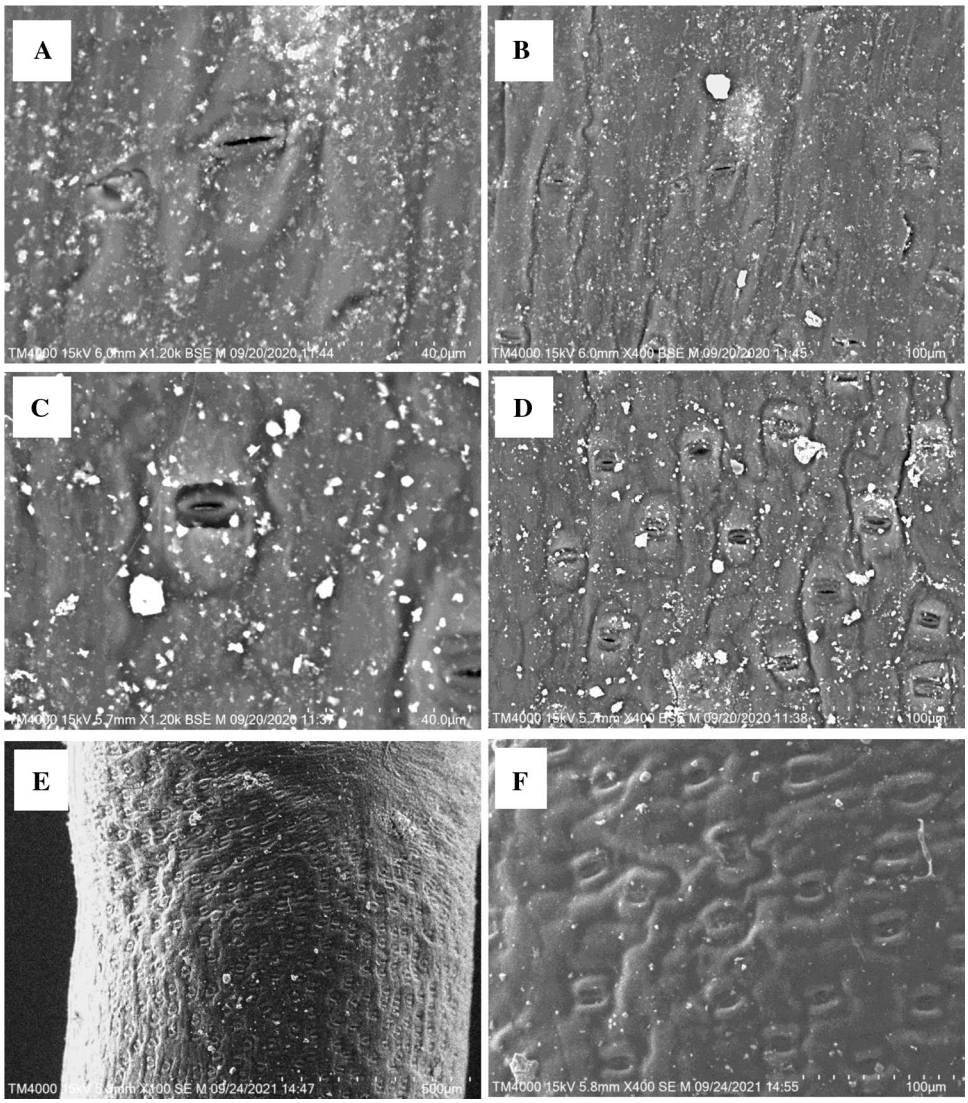


Fig. 9 Changes in epidermal microstructure of green assimilative branches of windward and leeward sides in *H. ammodendron* seedlings after sand-carrying wind blows of 12 m/s for 15 min. Small figures A and B are the windward sides of green assimilative branches, small figures C and D are the leeward sides, and small figures E and F are the controls from plants without wind erosion

time but non obvious difference in the sand-free wind group (Fig. 4C). Non-radiative energy dissipation in the PSII reaction center is the main means by which the photosynthetic apparatus eliminates excess excitation energy (Bilger and Björkman 1990; Elnour et al. 2018). The *NPQ* and the quantum yield of PSII photochemistry (Φ_{PSII}) were remarkably reduced in the sand-carrying wind group, which indicates that the PSII reaction center of *H. ammodendron* seedlings was more sensitive and easily affected, and the accumulation of excess excitation energy would damage the functional reaction center (Murchie and Niyogi 2011; Alencar et al. 2019). Furthermore, we divided the *NPQ* into rapidly and slowly relaxing quenching (NPQ_f and NPQ_s) using Maxwell and Johnson's (2000) method. Similar to the earlier result for alpine species of *Kobresia pygmaea* (Shi et al. 2015), the NPQ_f of *H. ammodendron* seedlings accounted for the majority component of PSII non-photochemical quenching. Limited by the in vitro measurement style, we finished 15 min of dark relaxation after a total of 30 min of low and high light illumination, so NPQ_f and NPQ_s were only comparable between the two wind erosion treatments and blowing times. It was clear that NPQ_f was sensitive to sustained sand-carrying wind erosion; compared to the sand-free wind, the sand-carrying wind group showed an obvious reduction in the NPQ_f/NPQ ratio and *NPQ*, which signifies that the photosynthetic apparatus was less likely to avoid potential photo-damage. The variation of *NPQ* involves O_2-dependent electron flow, proton gradient across thylakoid membrane (ΔpH), lutein cycle, inactivation of PSII reaction center, etc. (Baker 2008). The decrease in *NPQ* in sand-carrying wind was mainly due to the decrease in the NPQ_f component, which primarily relies on ΔpH.

In addition to the photochemical quenching of Φ_{PSII}, the excitation energy flux of the non-photochemical quenching reflecting competitive non-radiative thermal dissipation can be divided into two parts: the quantum yield of regulatory

energy dissipation Φ_{NPQ} and the quantum yield of non-regulatory energy dissipation Φ_{NO} (Kramer et al. 2004; Masahiro et al. 2016). Φ_{NPQ} represents the photo-induced down-regulatory process, and Φ_{NO} represents other non-photo-induced other energy losses (Baker and Rosenqvist 2004). Φ_{NPQ} and Φ_{NO} were used to analyze two aspects of the final destination of the excess excitation energy captured by PSII antenna pigments: regulation of light protective energy dissipation and difficulty regulating dissipation (Takahashi et al. 2010; Agrawal et al. 2016).

The analysis showed that the relative proportions of Φ_{PSII}, Φ_{NO}, and Φ_{NPQ} were affected by both wind erosion and light intensity. In the sand-free wind and sand-carrying wind groups, the relative proportions of the three components of Φ_{PSII}, Φ_{NO}, and Φ_{NPQ} at LL were approximately 5:2:3 and 5:3:2, respectively; at HL, they were approximately 2:2:6 and 2:3:5, respectively. Although the Φ_{PSII} was sensitive to light intensity, the proportion of Φ_{PSII} was almost the same in the two groups, which indicates that relative variation in excitation energy flux mainly occurred in Φ_{NPQ} and Φ_{NO} of non-photochemical quenching. Φ_{PSII} often showed a prominent difference between sand-free wind and sand-carrying wind; however, since the value was quite close, its proportion was relatively stable when analyzing the final destination of excitation energy flux. Compared to wind-only group, wind-blown sand caused a relative increase in Φ_{NO} and a relative decrease in Φ_{NPQ}. The Φ_{NO} value varied little by PPFD, and its ratio was roughly constant at LL and HL, accounting for approximately 2/10 under sand-free wind and 3/10 under sand-carrying wind, reflecting the characteristics of its non-photo-induced non-regulatory energy dissipation (Bellan et al. 2020) and its relative exacerbation of irreversible inactivation in the photosynthetic apparatus after exposure to sand-carrying wind. With prolonged of blowing time, sand-free wind also caused marked changes in Φ_{PSII}, Φ_{NO}, and Φ_{NPQ}, but the degree of variation and the fluctuation in the standard deviation of means were both far less than those in the sand-carrying wind group. This indicates that wind-blown sand increased the instability of photosynthetic function and had a more profound effect on the photosynthetic apparatus because of damage to the photosynthetic apparatus and its compensating effects. Continuous blowing of sand-carrying wind led to an obvious decrease in the *NPQ*, NPQ_f/NPQ ratio and Φ_{NPQ} components, which means that the ability to resist external adversity was reduced and that the physiological function of the photosynthetic apparatus was more likely to be inhibited or even damaged.

The maximum quantum efficiency of PSII photochemistry (F_v/F_m) is most frequently used as an indicator of photoinhibition or other injury to PSII complexes (Lucia et al. 2019; Pilarska et al. 2020). It is almost constant for many different plant species when measured under optimal conditions and its average approximately 0.83 to 0.85 (Björkman and Demmig 1987). Figure 6B compares the effects of sand-free wind and sand-carrying wind on F_v/F_m in the green assimilative branches of *H. ammodendron* seedlings and its relative change by blowing time. After continuous irradiation at 400 and 1500 μmol photons m^{-2} s^{-1} LL and HL for a total of 30 min, we further compared the F_v^r/F_m^r of dark relaxation for 15 min (Fig. 6A). The variation in F_v/F_m and F_v^r/F_m^r provides further verification of the analysis of PSII non-photochemical quenching. The results indicate that compared to sand-free wind, sustaining sand-carrying wind blowing caused a decrease in the performance of the PSII reaction center in *H. ammodendron* seedlings.

To determine whether strong light intensity aggravates the impacts of sand-carrying wind on PSII photochemical efficiency and non-photochemical quenching of green assimilative branches of *H. ammodendron* seedlings, we further analyzed the interaction of light intensity and duration of sand-carrying wind using multivariate GLM. Based on the variance analysis of the factorial experimental design, we further discuss the interactive effect of the duration of sand-carrying wind and light intensity. Table 1 shows that both blowing time and light intensity markedly affected q_{NP}, *NPQ*, Φ_{PSII}, Φ_{NO}, Φ_{NPQ}, and *rETR*, but their relative contributions to the total variation (η^2) were quite different. Light intensity was the main factor affecting Φ_{PSII}, Φ_{NPQ},

Table 1 Interactive effects of duration of sand-carrying wind and light intensity on chlorophyll fluorescence parameters in green branches of *H. ammodendron*

	Blowing time			Light intensity			Blowing time × Light intensity		
	F	Sig	η^2	F	Sig	η^2	F	Sig	η^2
q_{NP}	7.545	0.001	0.206	18.935	0	0.246	0.588	0.559	0.02
NPQ	9.431	0	0.245	16.325	0	0.22	0.101	0.904	0.003
Φ_{PSII}	10.711	0	0.27	2599.40	0	0.978	1.437	0.246	0.047
Φ_{NO}	6.986	0.002	0.194	8.512	0.005	0.128	0.007	0.993	0
Φ_{NPQ}	6.502	0.003	0.183	162.135	0	0.737	0.229	0.796	0.008
rETR	10.546	0	0.267	608.944	0	0.913	0.777	0.464	0.026

Note: F, Sig. and η^2 indicate the ratio of the average square, significant probability, and contribution to the total variation, respectively

and *rETR*, and their η^2 values were large. However, the η^2 values of q_{NP}, *NPQ*, and Φ_{NO} were similar and small, which indicates that the duration of sand-carrying wind and light intensity had roughly the same and smaller effects on the PSII non-photochemical quenching process and non-light-induced non-regulatory energy dissipation component. Table 1 also indicates that the significant probabilities (Sig.) were large, and the values of η^2 were small, indicating no interactive effects on blowing time and light intensity. The η^2 of Φ_{NO} was smaller in the light intensity, which also verifies its characteristics of non-light-induced non-regulation. As a process of unregulated energy dissipation in the form of non-light-induced energy loss, the Φ_{NO} was less affected by light intensity, and its value was dependent on the relative variation in Φ_{PSII} and Φ_{NPQ} (Baker 2008).

The interactive effect of two environmental factors is more popular in natural environments (Selda et al. 2021; Alauddin et al. 2021). This study showed that sand-carrying wind did not aggravate the impacts of strong light intensity on PSII photochemical efficiency or its non-photochemical quenching processes in assimilative branches of *H. ammodendron* seedlings. The interactive effect was not remarkable, and the effect of each factor was the result of superposition.

The analysis showed that during the experiments in the wind tunnel, sand particles were mainly concentrated at heights of less than 30 cm near the ground (especially below 10 cm), and the sand transport rate below 20 cm height was approximately 45 g cm^{-2} (Sun et al. 2021). Our observations indicated that the green assimilative branches of *H. ammodendron* seedlings were sporadically characterized by the phenomenon of wilting and/or withering, and this was particularly prominent in sand-carrying wind group. However, even in sand-free wind group, the phenomenon of water loss and wilting was occasionally incurred; but all these deficiencies could be restored to the normal growing status after one night of recovery except for wind-blown sand lasted for 40 min. Our similar research found that compared with the sand-free wind, the water content was reduced in a remarkable way after incurring blowing sand, in the meantime the photosynthetic activities of green assimilation branches were reduced (Shi et al. 2022); we believed that injury to the epidermis of tender branches by sand particles and augmentation of cuticle transpiration often generates a water imbalance. Li et al. (2019) also observed that mild and moderate sand-carrying wind could cause damage to the seedlings of eremophyte *Sarcozygium xanthoxylon* Bunge, but not necessarily osmotic stress; however, severe wind-blown sand could increase the activity of superoxide dismutase and catalase in leaves and their contents of soluble sugar and proline, which led to cell fluid outflow under osmotic stress.

The emergence of plants' physiological responses or symptoms usually requires some time, which often lags behind the environmental stimulus (De Roo et al. 2020; Chen et al. 2021). In contrast to the photosynthetic physiological response, the wither phenomenon of green assimilated branches appears only appeared a few hours later after wind-blown sand treatment (Zhao et al. 2017); observable scars on tender branches of seedlings also tend not to appear until the next day (Yu et al. 2002). Branches were seldom broken at 12 m/s wind speed, which may be related to the smaller crown of biennial plants and thinner lignified branches that are not very hard. The observation in the field after wind erosion does not confirm the speculation that the scars on the surface of the green branches would increase after sustained sand-carrying wind blowing. This may be due to the fact that when sand blows, the plant is relatively soft, and the tender branches can bend to be completely parallel to the wind direction, and the abrasive effect of sand grains does not increase much with the continuous erosion of wind. This is also the reason why the darkening occurred mostly at the base of assimilation branches and the windward side of branches (Fig. 8). However, scanning observations also showed that many dust adhered to the surface of tender green assimilative branches, even in control plants (Fig. 9). The adhering mounts of the windward side of the same branch are slightly higher than those of the leeward side, but the hypothesis that adhering mounts would increase with time of wind erosion is not confirmed. Larger particles of 10 to 15 μm were slightly rare on the branch surface; the most common particles were between 6 μm and 3 μm, and many very fine particles smaller than 3 μm also appeared.

Conclusions

The photosynthetic activities of *H. ammodendron* seedlings were remarkably impacted by sand-carrying wind simulated in the wind tunnel, which was mainly reflected in the following aspects:

1. *rETR* was restricted and obstructed by the sand-carrying wind, although no negative impact of sand-free wind.
2. The *NPQ* was sensitive to wind erosion, especially sand-carrying wind.
3. The photosynthetic apparatus was more likely to be inhibited or even damaged, manifested by the obvious reduction in the *NPQ*, NPQ_f/NPQ ratio and Φ_{NPQ} components after continuous blowing of sand-carrying wind.
4. The variation in F_v/F_m and F_v^r/F_m^r confirmed that sustaining sand-carrying wind blowing could cause a decrease in the performance of the PSII reaction center.
5. The exacerbation of irreversible inactivation in the photosynthetic apparatus after exposure to sand-carrying wind, manifested by the relative increasing of Φ_{NO} components.

Therefore, strong and frequent sandstorms in the early spring cause irreversible damage to the juvenile plants and result in an insufficient number of progeny and recruitment from seedlings into adults, restricting self-renewal and causing degradation of the *H. ammodendron* shelterbelt. In view of this, we considered that the artificial replenishment of healthier seedlings can be adopted measures in adult *H. ammodendron* shelter forests, where it is difficult to find regeneration seedlings, to compensate for the lack of survival of seed germination seedlings during natural regeneration.

Arid and desert areas of China are greatly affected by sandstorms almost every year, especially in early spring. The *Haloxylon ammodendron* has been considered as a preferred afforestation species for wind prevention and sand fixation; however, its population renewal is difficult and faced shrinkage or degeneration. Field observation found that it was not easy to see the juvenile seedlings in adult artificial shrub forests. Bormann and Likens (1981) considered that the survival of the population not only requires a suitable habitat environment, but also a sufficient number to reach the minimum population density; an insufficient number of progeny and recruitment from seedling into adults to maintain minimum population density may be a major reason limiting the self-renewal of plant populations and can even cause their degeneration. We supposed that the frequent sustained sandstorm in early spring led to irreversible damage to the photosynthetic physiological process, restricting survival of juvenile seedlings.

We carried out the simulation trials in the wind tunnel, took sand-free wind as a reference, combined with observation of morphological characteristics of epidermal tissue, the sensitive of green assimilative branches of seedlings to the sand-carrying winds was discussed. By means of analysis the results from rapid light response curves and steady-state light intensity, we found that PSII non-photochemical quenching process was more sensitive to wind erosion. We further analyzed the variations of components of PSII non-photochemical quenching and quantum yield of regulatory and non-regulatory energy dissipation. The results confirmed that sandstorm could result in irreversible inactivation of the PSII reaction centers of *H. ammodendron*.

Author contribution statement SBS: presided over the project execution, designed the experimental protocols, analyzed the data and drafted the manuscript. DWZ and RS: were responsible for the experimental design, participated in data analysis and paper revision. TS: was responsible for field plant cultivation and the wind tunnel erosion trials. FLW and XZG: carried out the laboratory experimental items. YNZ, PZ and GXX: participated in field plant cultivation and wind tunnel erosion trials. JNT: participated in the discussion of overall trials design and paper revision. All authors read and approved the manuscript.

Acknowledgements We thank Profs. Caizhou Kang and Kejie Zhan (Gansu Desert Control Research Institute, China), who provided warm help with daily field management and statistical analysis. This work was financially supported by the National Natural Science Foundation of China (31660237), the Science Foundation of Qinghai Province (2019-ZJ-7016), and the Construction Project for Innovation Platform of Qinghai Province (2017-ZJ-Y20, 2017-ZJ-Y14).

Data availability statement The data sets generated in this study are available on request to the corresponding author.

Declarations

Conflict of interest The authors declare that they have no conflicts of interest.

Open Access This article is licensed under a Creative Commons Attribution 4.0 International License, which permits use, sharing, adaptation, distribution and reproduction in any medium or format, as long as you give appropriate credit to the original author(s) and the source, provide a link to the Creative Commons licence, and indicate if changes were made. The images or other third party material in this article are included in the article's Creative Commons licence, unless indicated otherwise in a credit line to the material. If material is not included in the article's Creative Commons licence and your intended use is not permitted by statutory regulation or exceeds the permitted use, you will need to obtain permission directly from the copyright holder. To view a copy of this licence, visit http://creativecommons.org/licenses/by/4.0/.

Open Access This article is licensed under a Creative Commons Attribution 4.0 International License, which permits use, sharing, adaptation, distribution and reproduction in any medium or format, as long as you give appropriate credit to the original author(s) and the source, provide a link to the Creative Commons licence, and indicate if changes were made. The images or other third party material in this article are included in the article's Creative Commons licence, unless indicated otherwise in a credit line to the material. If material is not included in the article's Creative Commons licence and your intended use is not permitted by statutory regulation or exceeds the permitted use, you will need to obtain permission directly from the copyright holder. To view a copy of this licence, visit http://creativecommons.org/licenses/by/4.0/.

References

Agrawal D, Allakhverdiev SI, Jajoo A (2016) Cyclic electron flow plays an important role in protection of spinach leaves under high temperature stress. Russ J Plant Physiol 63(2):210–215

Alauddin M, Mohsin GM, Ali AHMZ, Rahman MK (2021) Interactive effects of rice bran compost and chemical fertilizers on macronutrients, oil and protein content in sunflower (*Helianthus annuus* L.). Int J Agric Res Innov Technol 10(2):91–99

Alencar VTCB, Lobo AKM, Silveira JAG (2019) High ammonium supply impairs photosynthetic efficiency in rice exposed to excess light. Photosynth Res. https://doi.org/10.1007/s11120-019-00614-z

Baker NR (2008) Chlorophyll fluorescence: a probe of photosynthesis in vivo. Annu Rev Plant Biol 59:89–113

Baker NR, Rosenqvist E (2004) Application of chlorophyll fluorescence and improve crop production strategies: an examination of future possibilities. J Exp Bot 55:1607–1621

Bellan A, Bucci F, Perin G, Alboresi A, Morosinotto T (2020) Photosynthesis regulation in response to fluctuating light in the secondary endosymbiont alga nannochloropsis gaditana. Plant Cell Physiol 61(1):41–52

Bilger W, Björkman O (1990) Role of the xanthophyll cycle protoprotection elucidated by measurements of light-induced absorbance changes, fluorescence and photosynthesis in leaves of *Hedera canariensis*. Photosynth Res 25:173–185

Björkman O, Demmig B (1987) Photon yield of O_2 evolution and chlorophyll fluorescence characteristics at 77 K among vascular plants of diverse origins. Planta 170:489–504

Bormann FH, Likens GE (1981) Pattern and Process in a Forested Ecosystem. Springer-Verbag, Heidelberg

Chen WQ, Jl D, Tan J, Zhang JY, Liu BH (2018) Desertification change in Central Asia based on DPM-SPOT from 2000 to 2015. Arid Land Geography 41(1):119–127

Chen WY, Jia B, Chen JY, Feng YJ, Li Y, Chen MT, Liu HH, Yin ZT (2021) Effects of different planting densities on photosynthesis in maize determined via prompt fluorescence, delayed fluorescence and P700 signals. Plants 10(2):276–283

De Roo L, Salomón RL, Oleksyn J, Steppe K (2020) Woody tissue photosynthesis delays drought stress in Populus tremula trees and maintains starch reserves in branch xylem tissues. New Phytol 228(1):70–81

Ding F, Ji RF, Chen F, Zhang JC, Liu YJ, Wang FL (2011) Spatial distributing character of *Haloxylon ammodendron* seedling growth in Minqin. J Gansu Forest Sci Technol 36:7–12

Dong ZB, Chen GT, He XD, Han ZW, Wang XM (2004) Controlling blown sand along the highway crossing the Taklimakan Desert. J Arid Environ 57:329–344

Dyer MI, Turner CL, Seastedt TR (1991) Mowing and fertilization effect on productivity and spectral reflectance in Bromus inermis plots. Ecol Appl 1:443–452

Edelfeldt S, Bengtsson K, Dahlgren PJ (2019) Demographic senescence and effects on population dynamics of a perennial plant. Ecology 100(8):e02742. https://doi.org/10.1002/ecy.2742

Elnour MAMH, Dietzel L, Ramanan C, Büchel C, van Grondelle R (2018) Energy dissipation mechanisms in the FCPb light-harvesting complex of the diatom *Cyclotella meneghiniana*. Biochimica et Biophysica Acta (BBA). Bioenergetics 10:1151–1160

Gaudet CI, Keddy PA (1998) A comparative approach to predicting competitive ability from plant traits. Nature 334:242–243

Genty B, Briantais JM, Baker NR (1989) The relationship between the quantum yield of photosynthetic electron transport and quenching of chlorophyll fluorescence. BBA-Gen Subjects 990:87–92

Guo QS, Guo ZH, Yan H, Wang CL, Tang DY, Ma C, He HY (2005) Study on potential distribution of *Haloxylon* plants dominated desert vegetation in China. Acta Ecologica Sinica 25, 848–853+946

He YP, Zhang YW, Gu ZL (2021) Research progress of very strong sandstorm and its future research prospects. China Environ Sci 41(8):3511–3522

Hu D, Lv GH, Qie YD, Wang HF, Yang F, Jiang LM (2021) Response of morphological characters and photosynthetic characteristics of *Haloxylon ammodendron* to water and salt stress. Sustainability 13(1):388–388

Kramer DM, Johnson G, Kiirats O, Edwards GE (2004) New fluorescence parameters for the determination of Q_A redox state and excitation energy fluxes. Photosynth Res 79:209–218

Li DM, Ji YF, Zhang YH, Wei LY, Wang F, Ma R, Jiang ZR (2019) Effects of wind-drift sand on physiological characteristics of *Zygophyllum xanthoxylum* seedling. J Northwest A&F University (Nat Sci Ed) 47(3): 103–110

Lucia G, Ermes LP, Marco L (2019) Chlorophyll fluorescence, photoinhibition and abiotic stress: does it make any difference the fact to be a C_3 or C_4 species? Front Plant Sci 10:174. https://doi.org/10.3389/fpls.2019.00174

Ma YC, Li YY, Yang JP, Zeng T, Zhang AP, Zhang CY (2019) Relationships between boundary layer height and different disaster weathers in north-central Qinghai Province. Plateau Meteorol 38(5):1048–1057. https://doi.org/10.7522/j.issn.1000-0534.2018.00136

Masahiro M, Hiroshi K, Tatsuya T, Kintake S (2016) Relationship between photochemical quenching and non-Photochemical quenching in six species of cyanobacteria reveals species difference in redox state and species commonality in energy dissipation. Plant Cell Physiol 61(1), 57(7), 1510–1517

Masini L, Grenville-Briggs LJ, Andreasson E, Råberg L, Lankinen Å (2019) Tolerance and overcompensation to infection by *Phytophthora infestans* in the wild perennial climber *Solanum dulcamara*. Ecol Evol 9(8):4557–4567

Maxwell K, Johnson GN (2000) Chlorophyll fluorescence – a practical guide. J Exp Bot 51:659–668

Murchie EH, Niyogi KK (2011) Manipulation of photoprotection to improve plant photosynthesis. Plant Physiol 155:86–92

Niyogi KK, Truong TB (2013) Evolution of flexible non-photochemical quenching mechanisms that regulate light harvesting in oxygenic photosynthesis. Curr Opin Plant Biol 16:307–314

Oxborough K, Baker NR (1997) Resolving chlorophyll *a* fluorescence images of photosynthetic efficiency into photochemical and non-photochemical components: calculation of q_P and F_v'/F_m' without measuring F_o'. Photosynth Res 54:135–142

Pilarska M, Niewiadomska E, Sychta K, Słomkal A (2020) Differences in the functioning of photosynthetic electron transport between metallicolous and non-metallicolous populations of the pseudometallophyte *Viola tricolor*. J Plant Physiol. https://doi.org/10.1016/j.jplph.2020.153185

Pleban JR, Guadagno CR, Mackay DS, Weinig C, Ewers BE (2020) Rapid chlorophyll *a* fluorescence light response curves mechanistically inform photosynthesis modeling. Plant Physiol (bethesda) 183(2):602–619

Qian ZA, Song MH, Li WY (2002) Analyses on distributive variation and forecast of sand-dust storms in recent 50 years in north China. J Desert Res 22:106–111

Qu JJ, Ling YQ, Liu BJ, Chen GT, Wang T, Dong ZB (2019) Research status and development trends of wind-sand engineering in China. Adv Earth Sci 34:225–231

Quick WP, Stitt M (1989) An examination of factors contributing to non-photochemical quenching of chlorophyll fluorescence in barley leaves. Biochem Biophys Acta 977:287–296

Selda O, Melek E, Ertan Y, Ustun S, Metin T, Atilla D (2021) Interactive effects of salinity and drought stress on photosynthetic characteristics and physiology of tomato (*Lycopersicon esculentum* L.) seedlings. S Afr J Bot 137:335–339

Serôdio J, Vieira S, Cruz S, Coelho H (2006) Rapid light-response curves of chlorophyll fluorescence in microalgae: relationship to steady-state light curves and non-photochemical quenching in benthic diatom-dominated assemblages. Photosynth Res 90(1):29–43

Shi PJ, Yan P, Gao SY, Wang YM, Ha S, Yu YJ (2000) The duststorm disaster in China and its research progress. J Natl Disasters 9:71–77

Shi SB, Li TC, Li M, Liu SZ, Li AD, Ma JP (2015) Interaction effect analysis of soil-drought and strong light on PSII non-photochemical quenching in *Kobresia pygmaea* leaves. Plant Physiol J 51:1678–1686

Shi SB, Zhou DW, Wang FL, Shi R, Sun T, Li TC, Ma JL, Wan X, Ma JP, Tang JN (2022) Sandstorms cause shrinkage of *Haloxylon ammodendron* shrubs and limit their self-renewal.

Theoret Experim Plant Physiol. https://doi.org/10.1007/s40626-022-00242-4

Song YY, Li YY, Zhang WH (2010) Analysis of spatial pattern and spatial association of *Haloxylon ammodendron* population in different developmental stages. Acta Ecol Sin 30:4317–4327

Štroch M, Kuldová K, Kalina J, Špunda V (2008) Dynamics of the xanthophyll cycle and non-radiative dissipation of absorbed light energy during exposure of Norway spruce to high irradiance. J Plant Physiol 165(6):612–622

Su YZ, Liu TN, Kong JQ (2019) The establishment and development of *Haloxylon ammodendron* promotes salt accumulation in surface soil of arid sandy land. Scie Cold Arid Regions 11(2):116–125. https://doi.org/10.3724/SP.J.1226.2019.00116

Sun T, Ma JP, Shi SB, Han FG, Zhang YN, Wang FL, Wan X, Zhang HY (2021) Effect on the phenotype of *Haloxylon ammodendron* by wind sand-blown stress simulated in the wind tunnel. Forest Environm Sci 34(7):7–14

Takahashi S, Milward SE, Yamori W, Evans JR, Hillier W, Badger MR (2010) The solar action spectrum of photosystem II damage. Plant Physiol 153:988–993

Wan W, Yan CZ (2018) Research progress of eco-environmental degradation in Alxa Plateau. J Earth Environm 9(2):109–122

Wang RP, Li L (2008) The extinction vortex of small population. J Biol 25(6):14–16

Wang JH, Ma QL (2003) Study on restoration strategies, characteristics and status of degenerated artificial *Haloxylon ammodendron* communities at the edge of Minqin oasis. Acta Botan Boreali-Occiden Sin 23:2107–2112

Wang T, Chen GT, Zhao HL, Dong ZB, Zhang XY, Zheng XJ, Wang NA (2006) Research progress on Aeolian desertification process and controlling in north of China. J Desert Res 26:507–516

Xu XB, Peng KS, Hu PH, Liu YF (2002) The damage of sandstorm to development of west China and its harnessing counter measures. J Chongqing University (social Sciences Edition) 8:1–8

Yu JY, Shi PJ, He LP, Liu JQ (2002) Research on the effects of wind-sand current on the plant growth. Adv Earth Sci 17:262–267

Zhang KC, Qu JJ, Liao KT, Niu QH, Han QJ (2010) Damage by wind-blown sand and its control along Qinghai-Tibet Railway in China. Aeol Res 1:143–146

Zhao SX, Sun JH (2013) Study on the mechanism and prediction of disastrous weather during recent years. Chin J Atmos Sci 37:297–312

Zhao HL, Li J, Zhou RL, Yun JY, Feng J, Sun N (2017) Effects of brief sand-drift wind blowing on photosynthesis and transpiration properties of *Pinus sylvestris* var. *mogolica* seedling. J Desert Res 37:254–260

Publisher's Note Springer Nature remains neutral with regard to jurisdictional claims in published maps and institutional affiliations.